Indian Journal of Chemistry
Vol. 63, January 2024, pp. 57-64
DOI: 10.56042/ijc.v63i1.3247

Influence of temperature and solvents on the molecular interactions of benzo[*d*]imidazole substituted 1,3,4-oxadiazole derivatives

D R Godhani*, A H Saiyad, J P Mehta & U P Mehta
Department of Chemistry (DST-FIST sponsored Department),
Mahatma Gandhi Campus, Maharaja Krishnakumarsinhji Bhavnagar University, Bhavnagar 364 002, India
E-mail: drgodhani@mkbhavuni.edu.in

Received 26 June 2023; accepted (revised) 22 December 2023

Thermo-acoustical parameters of solutions of (2-[(5-(4-nitrophenyl)-1,3,4-oxadiazol-2-ylthio)methyl]-1*H*-benzo[*d*]imidazol-1-yl)(phenyl)methanone, (AS_2-13) and (2-[(5-(4-aminophenyl)-1,3,4-oxadiazol-2-ylthiomethyl]-1*H*-benzo[*d*]imidazol-1-yl)(phenyl)methanone, (AS_2-14) in dimethyl sulfoxide (DMSO) and *N, N*-dimethylformamide (DMF) have been evaluated. Various acoustical and thermodynamic parameters, including density (ρ), viscosity (η), and ultrasonic sound velocity (U), have been measured at three different temperatures, namely (298.15 K, 308.15 K and 318.15 K at atmospheric pressure. These results have been explained by considering the molecular interactions of the liquid mixture's components.

Keywords: 1,3,4-Oxadiazole, Ultrasonic sound velocity, Density, Acoustical parameter, Thermodynamic parameters, Molecular interaction

After the synthesis knowing the physicochemical properties of a pharmacologically active compound is essential for developing a medicine with the best possible mechanism of action and long-term stability[1]. Ultrasonic sound velocity is a broad field of study that has applications in geology, geography, biology, biochemistry, the polymer industry, medicine, and engineering[2]. The ultrasonic technique has innumerable applications in various fields[3-6]. Multiple information about intermolecular forces and bulk properties is represented by the ultrasonic sound velocity(U),viscosity (η),density(ρ)[7,8] which is employed in a variety of industrial and manufacturing processes.Ultrasonic sound velocity is also used in the pharmaceutical industry[9]. Ultrasonic sound velocity is used in synthetic chemistry to reduce reaction temperature, increase yield, shorten reaction time, and predict phase transition materials, among other things[10]. In addition, ultrasonic sound velocity measurements are used to investigate the nature of molecular interactions in a variety of binary and ternary liquid mixtures[11-13]. This approach had been used by numerous researchers for solutions of the polymer[14], other electrolytes[15], and non-electrolytes[16]. 1,3,4-oxadiazole moiety has many biological applications such as show antitumor[17], anti-inflammatory[18], antidepressant[19], antimalarial[20], anti-HIV[21], antimicrobial[22], antibacterial[23], antifungal[24], antiviral[25], antidiabetic[26], anticancer[27], diuretic[28], *etc*.

Thus, in this section, ultrasonic studies of both the synthesized compound (2-[(5-(4nitrophenyl)-1,3,4-oxadiazol-2-ylthio)methyl]-1*H*-benzo[*d*]imidazol-1-yl)(phenyl)methanone, (AS_2-13) and (2-[(5-(4-aminophenyl)-1,3,4-oxadiazol-2-ylthio)methyl]-1*H*-benzo[*d*]imidazol-1-yl)(phenyl)methanone, (AS_2-14) have been done in DMF (*N, N* dimethylformamide) and DMSO (dimethyl sulfoxide) solutions at different temperatures (298.15 K - 318.15 K) in order to study molecular interactions in these solution.

Experimental Section

The solvents DMSO (dimethyl sulfoxide) and DMF (*N,N*-dimethyl formamide) used in the current study were of AR grade supplied by Spectrochem Pvt. Ltd. and all the chemicals used in the synthesis were of analytical grade with on purity of 99.7% were used as such without further purification. Aluminum-coated plate Ge160F254 was the material of the TLC plates. The (2-[(5-(4nitrophenyl)-1,3,4-oxadiazol-2-ylthio)methyl]-1*H*-benzo[*d*]imidazol-1-yl)(phenyl) methanone, (AS_2-13) and (2-[(5-(4-aminophenyl)-1,3,4-oxadiazol-2-ylthio)methyl]-1*H*-benzo[*d*]imidazol-1-yl)(phenyl)methanone,(AS_2-14) used in this analysis was manufactured in our laboratory. The structure of the present synthesized compounds (AS_2-13) and (AS_2-14) is shown in Fig. 1.

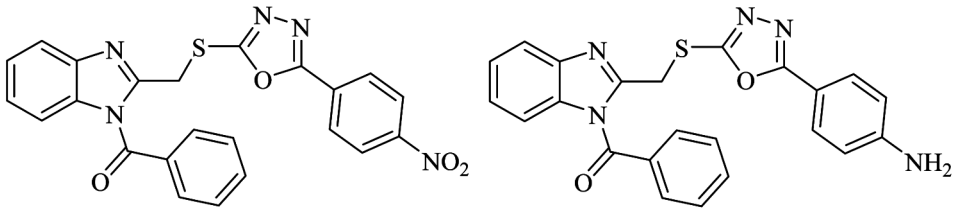

Fig. 1 — Structure of (2-([5-(4-nitrophenyl)-1,3,4-oxadiazol-2-ylthio)methyl]-1*H*-benzo[*d*]imidazol-1-yl)(phenyl)methanone, (AS_2-13) and (2-([5-(4-aminophenyl)-1,3,4-oxadiazol-2-ylthio)methyl]-1*H*-benzo[*d*]imidazol-1-yl)(phenyl)methanone, (AS_2-14).

Table 1 — Comparison of measured density, ρ, viscosity, η, and ultrasonic sound velocity, U data for pure DMSO and DMF with literature values at T = (298.15, 308.15 and 318.15) K.

Solvent	This work			Literature		
	T = 298.15 K	T = 308.15 K	T = 318.15 K	T = 298.15 K	T = 308.15 K	T = 318.15 K
ρ / (kg · m^{-3})ρ / (kg · m^{-3})						
DMSO	1094.77	1085.21	1075.19	1095.29[34]	1085.25[34]	1075.21[34]
DMF	948.02	938.93	928.87	943.94[37]	934.64[37]	925.80[37]
η / (mPa ·s) η / (mPa · s)						
DMSO	1.8556	1.4578	1.2487	1.8480[34]	1.4980[34]	1.310[35]
DMF	0.8169	0.7246	0.5947	0.8040[39]	0.7103[38]	0.6348[38]
U / (m · s^{-1})U / (m · s^{-1})						
DMSO	1484.55	1452.05	1418.72	1485.1[36]	1451.3[36]	1417.7[36]
DMF	1461.50	1420.25	1379.14	1457.49[37]	1418.95[37]	1379.60[40]

Density, viscosity, and Ultrasonic sound velocity, measurements in pure solvents (DMF and DMSO) and solutions of both the compound (0.001-0.010 mol·kg^{-1}) in DMF and DMSO were made at three different temperatures *viz*. (298.15, 308.15 and 318.15) K by using an ultrasonic sound velocity meter Anton Paar DSA 5000 M. The temperature was controlled by the digital temperature controller of the Instrucare solution viscosity bath with an accuracy of 0.5 °C. For density measurement, the Anton paar density meter (DSA 5000M) was used. Fungilab viscolead advance viscometer was used for the viscosity measurement. Ultrasonic sound velocity (U), density (ρ), and viscosity (η) measurements were accurate to ±1%, ±0.0002 g·cm^{-3} and ±0.40% respectively. The uncertainty of temperature is ±0.1K and that of concentration measured is ±0.001mol·dm^{-3}. To establish their solubility at the temperature, all of the samples were prepared freshly using Sonixvibra-cells (VCX500) and kept there for 24 hours. Samples were preserved in bottles under a vacuum until further use. Using standard equations, many acoustical factors are estimated from the experimental data of, ρ, η and U[29-33].

Results and Discussion

Dimethyl sulfoxide (DMSO) and *N,N*-dimethyl-formamide (DMF) used in the current study were compared to the standard data for ultrasonic sound velocity (U), density (ρ), and viscosity (η) in Table 1. Which denotes a satisfactory alignment of empirical and theoretical data. The results also indicated that our experiments were perfectly calibrated and standardized. The ρ, η and U of pure solvents and solutions of AS_2-13 and AS_2-14 in DMSO and DMF were measured at T = (298.15, 308.15 and 318.15) K and are specified in Table 2 and Table 3. Here Table 4, Table 5, Table 6 and Table 7 clearly shows that, ρ, η and U increased with concentration (C) and decreased with temperature (T). Least squares analysis was used to test the concentration and temperature dependence of these data. The experimental correlation between ρ and C are R^2 = 0.852-0.9959, η and $C$are R^2 = 0.9246-0.9979 and U and C are R^2 = 0.935-0.9827 which indicates a fair to excellent linear relationship between the variables under study, as displayed in Fig. 2, Fig. 3 and Fig. 4. Increasing ρ, η and U with C show that cohesive forces increased as a result of strong molecular interactions, while decreasing ρ, η and U with

T show that cohesive forces decreased. Structure formation (intermolecular association) and structure destruction are the opposing effects of rising temperature. The tendency for structures to form is primarily caused by interactions between solutes-solvents, whereas structures that have already been formed are disrupted by thermal fluctuations. When the thermal energy exceeds the interaction energy, the destruction of previously formed structure. The -NO_2 and -NH_2 group of the structure (AS_2-13 and AS_2-14) are polar groups, which form associations with solvent molecules and thus have a tendency to form structures in the system. With the electronegative groups of the solvents, the molecule's -NO_2 group is likely to form a hydrogen bond. *i.e*. lone pairs of electrons of DMSO and DMF, while -NH_2 group may undergo hydrogen bond formation with DMF. As a result, dipole-dipole interactions of opposite types favor the formation of structures while interactions of the same type result in the destruction of previously formed structures. It is shown by the findings that interactions between dipoles of different types predominate over those of the same types. Therefore, an increase in T favors an increase in kinetic energy and volume expansion, which causes a decrease in ρ and η to be seen. The density and viscosity of medium, pressure, temperature, *etc*. effect on the ultrasonic sound velocity. To comprehend the impact of concentration, temperature, the type of solvents used, and the structures of AS_2-13 and AS_2-14 on the tendency to form or break structures, a number of acoustical factors, including acoustical impendence (Z), isentropic compressibility (κ_S), free volume (V_f), Rao's molar sound function (R_m), Van der Waals constant (b), intermolecular free path length (L_f), internal pressure (π), and viscous relaxation time (τ) were determined by using the experimental data of ρ, η and U of AS_2-13 and AS_2-14 in DMSO and DMF solutions at three temperatures according to standard equations. The concentration and temperature dependence of acoustical parameters reveals a wealth of knowledge regarding the strength of interactions between molecules in solutions of AS_2-13 and AS_2-14.

Table 2 — The density, ρ, viscosity, η, and ultrasonic sound velocity, U, for AS_2-13 in DMSO and DMF solutions at T = (298.15, 308.15 and 318.15) K and at atmospheric pressure.

DMSO +AS_2-13 system				DMF + AS_2-13 system			
$m^a \cdot 10^{-3}$/ (mol· kg^{-1})	ρ / (kg · m^{-3})	η / (mPa · s)	U / (m · s^{-1})	$m^a \cdot 10^{-3}$ / (mol· kg^{-1})	ρ / (kg · m^{-3})	η / (mPa · s)	U / (m · s^{-1})
T = 298.15 K				T = 298.15 K			
0	1094.77	1.8556	1484.55	0	948.02	0.8169	1461.5
0.9124	1096.45	1.9546	1485.98	1.0456	956.81	0.8503	1462.18
1.8244	1097.17	2.0015	1486.49	2.0869	959.28	0.8676	1463.37
3.6490	1098.01	2.0525	1487.31	4.1684	961.42	0.8753	1464.2
5.4747	1098.69	2.1289	1488.01	6.2427	963.87	0.9072	1466.84
7.2974	1099.93	2.1713	1488.84	8.3288	964.18	0.9169	1468.57
9.1248	1100.01	2.209	1491.06	10.3950	966.57	0.9343	1469.61
T = 308.15 K				T = 308.15 K			
0	1085.21	1.4578	1452.05	0	938.93	0.7246	1420.25
0.9207	1086.56	1.50014	1453.13	1.0586	945.13	0.7619	1422.45
1.8404	1087.63	1.5296	1454.09	2.1125	947.65	0.7723	1423.78
3.6794	1088.96	1.5702	1455.43	4.2266	948.21	0.7814	1425.88
5.5217	1089.36	1.6389	1456.36	6.3332	950.13	0.8018	1426.89
7.3643	1089.98	1.6767	1457.85	8.4426	951.23	0.8134	1428.21
9.2056	1090.87	1.7099	1458.04	10.5387	953.45	0.8203	1429.67
T = 318.15 K				T = 318.15 K			
0	1075.19	1.2487	1418.72	0	928.87	0.5947	1379.14
0.9283	1077.74	1.3056	1420.6	1.0752	930.51	0.6327	1383.25
1.8566	1078.15	1.3301	1420.9	2.1456	933.07	0.6421	1386.01
3.7131	1079.09	1.3589	1421.36	4.2746	937.59	0.6854	1387.56
5.5676	1080.41	1.3904	1422.3	6.4001	940.23	0.6901	1388.89
7.4210	1081.68	1.4256	1423.77	8.5285	941.69	0.7028	1390.78
9.2758	1082.65	1.4599	1424.45	10.6586	942.78	0.7197	1391.78

[a] Molality of AS_2-13 in DMSO and DMF solutions at different temperatures in mol· kg^{-1}.

Table 3 — The density, ρ, viscosity, η, and ultrasonic sound velocity, U, for AS_2-14 in DMSO and DMF solutions at T = (298.15, 308.15 and 318.15) K and at atmospheric pressure.

DMSO + AS_2-14 system				DMF + AS_2-14 system			
$m^a \cdot 10^{-3}$/ (mol· kg^{-1})	ρ / (kg · m^{-3})	η / (m Pa ·s)	U / (m · s^{-1})	$m^a \cdot 10^{-3}$ / (mol· kg^{-1})	ρ / (kg · m^{-3})	η / (mPa · s)	U / (m · s^{-1})
T = 298.15 K				T = 298.15 K			
0	1094.77	1.8556	1484.55	0	948.02	0.8169	1461.5
0.9130	1095.69	1.8703	1485.97	1.0468	955.69	0.8414	1461.89
1.8262	1096.02	1.9418	1486.06	2.0892	958.18	0.8576	1462.18
3.6524	1096.89	2.0518	1487.33	4.1731	960.23	0.8608	1463.72
5.4815	1097.15	2.1318	1488.51	6.2486	962.78	0.8934	1465.43
7.3084	1098.05	2.2687	1489.91	8.3299	963.81	0.9045	1467.8
9.1279	1099.81	2.3401	1491.72	10.4003	965.78	0.9104	1468.33
T = 308.15 K				T = 308.15 K			
0	1085.21	1.4578	1452.05	0	938.93	0.7246	1420.25
0.9209	1086.31	1.5318	1452.3	1.0606	943.31	0.7491	1421.02
1.8392	1088.29	1.5603	1453.86	2.1205	944.04	0.7613	1421.87
3.6772	1089.49	1.6218	1454.68	4.2289	947.59	0.7804	1422.12
5.5180	1089.92	1.6801	1455.08	6.3394	949.03	0.7989	1423.56
7.3623	1090.03	1.7211	1455.93	8.4476	950.43	0.8085	1425.43
9.1986	1091.39	1.741	1456.87	10.5503	952.11	0.8197	1427.28
T = 318.15 K				T = 318.15 K			
0	1075.19	1.2487	1418.72	0	928.87	0.5947	1379.14
0.9295	1076.32	1.3053	1419.12	1.0768	929.41	0.6272	1380.58
1.8569	1077.91	1.3583	1420.09	2.1499	931.11	0.6304	1381.78
3.7157	1078.23	1.4058	1421.67	4.2825	935.75	0.6645	1382.21
5.5738	1079.03	1.4671	1422.01	6.3920	941.23	0.6811	1384.69
7.4324	1079.78	1.4889	1422.78	8.5150	942.93	0.7018	1386.24
9.2830	1081.51	1.5421	1424.33	10.6420	943.87	0.7141	1388.97

[a] Molality of AS_2-14 in DMSO and DMF solutions at different temperatures in mol· kg^{-1}.

Table 4 — The least-square equations and regression coefficients for AS_2-13 solutions in DMSO at T = (298.15, 308.15 and 318.15) K.

Parameter	Least square equations (regression coefficients, R^2)		
	T = 298.15 K	T = 308.15 K	T = 318.15 K
ρ /(kg · m^{-3})	y = 408.22x + 1096.3 R² = 0.9672	y = 438.36x + 1086.6 R² = 0.9465	y = 562.96x + 1077 R² = 0.9959
η / (mPa · s)	y = 28.207x + 1.9402 R² = 0.9826	y = 23.913x + 1.4807 R² = 0.9887	y = 16.713x + 1.2921 R² = 0.9979
U / (m · s^{-1})	y = 512.58x + 1485.3 R² = 0.9463	y = 560.11x + 1452.9 R² = 0.9677	y = 446.63x +1419.9 R² = 0.9718
$Z \cdot 10^6$ / (kg · m^{-2} · s^{-1})	y = 1.1705x + 1.6283 R² = 0.9956	y = 1.248x + 1.5788 R² = 0.967	y = 1.2832x +1.5293 R² = 0.9901
$\kappa_s \cdot 10^{-10}$ /(Pa^{-1})	y = -4.3522x + 4.1347 R² = 0.9884	y = -5.0826x + 4.3594 R² = 0.9689	y = -5.2593x + 4.6049 R² = 0.9874
$L_f \cdot 10^{-11}$ /(m)	y = -2.2507x + 4.2575 R² = 0.9885	y = -2.5545x + 4.3716 R² = 0.9691	y = -2.5733x + 4.493 R² = 0.9863
$R_m \cdot 10^{-4}$ / (m$^{10/3}$ · s$^{-1/3}$ ·mol^{-1})	y = -1.7283x + 8.1296 R² = 0.8422	y = -1.87x + 8.1416 R² = 0.8779	y = -3.0244x + 8.1514 R² = 0.9969
$b \cdot 10^{-5}$ /(m^3)	y = -2.2693x + 7.0265 R² = 0.9561	y = -2.5019x + 7.0858 R² = 0.9318	y = -3.3701x + 7.1459 R² = 0.9953
$\pi \cdot 10^8$ /(Pa)	y = 54.286x + 7.7146 R² = 0.9785	y = 54.464x + 7.0021 R² = 0.988	y = 43.45x + 6.7899 R² = 0.998
$V_f \cdot 10^{-7}$ /(m^3)	y = -9.3124x + 0.5198 R² = 0.9701	y = -14.673x + 0.7531 R² = 0.9821	y = -14.376x + 0.8942 R² = 0.9956
$\tau \cdot 10^{-13}$ /(s)	y = 142.48x + 10.699 R² = 0.9768	y = 127.3x + 8.6092 R² = 0.9875	y = 92.265x + 7.9356 R² = 0.9972
S_n	y = 2E+09x^4 - 5E+07x^3 + 413520 x^2 - 418.5x + 0.7069 R² = 0.9955	y = 1E+09x^4 - 3E+07x^3 + 299330x^2 - 625.21x + 1.2622 R² = 1	y = 6E+12x^5 - 2E+11x^4 + 2E+09x^3 - 1E+07x^2 + 24584x - 15.941 R² = 1

Table 5 — The least-square equations and regression coefficients for **AS_2-14** solutions in DMSO at T = (298.15, 308.15 and 318.15) K.

Parameter	Least square equations (regression coefficients, R^2)		
	T = 298.15 K	T = 308.15 K	T = 318.15 K
ρ /(kg · m^{-3})	y = 417.07x + 1095.1 R² = 0.9383	y = 462.27x + 1086.8 R² = 0.852	y = 491.23x + 1076.3 R² = 0.9395
η / (mPa · s)	y = 52.262x + 1.8307 R² = 0.9936	y = 24.26x + 1.5173 R² = 0.9747	y = 24.896x + 1.2993 R² = 0.9752
U / (m · s^{-1})	y = 644.38x + 1484.9 R² = 0.9827	y = 443.4x + 1452.5 R² = 0.9353	y = 524.6x + 1419 R² = 0.961
$Z \cdot 10^6$ / (kg · m^{-2} · s^{-1})	y = 1.3281x + 1.6262 R² = 0.9687	y = 1.1553x + 1.5786 R² = 0.8933	y = 1.2644x + 1.5272 R² = 0.9604
$\kappa_s \cdot 10^{-10}$ /(Pa^{-1})	y = -5.1279x + 4.1411 R² = 0.9759	y = -4.4888x + 4.3611 R² = 0.9072	y = -5.4712x + 4.6146 R² = 0.9641
$L_f \cdot 10^{-11}$ /(m)	y = -2.6443x + 4.2608 R² = 0.9756	y = -2.2551x + 4.3724 R² = 0.9068	y = -2.675x + 4.4977 R² = 0.9635
$R_m \cdot 10^{-4}$ / (m$^{10/3}$ · s$^{-1/3}$ ·mol^{-1})	y = -1.5856x + 8.1374 R² = 0.8439	y = -2.2924x + 8.1392 R² = 0.7722	y = -2.3695x + 8.1555 R² = 0.8858
$b \cdot 10^{-5}$ /(m^3)	y = -2.3466x + 7.0339 R² = 0.9228	y = -2.6876x + 7.0844 R² = 0.8223	y = -2.9241x + 7.151 R² = 0.9268
$\pi \cdot 10^8$ /(Pa)	y = 99.597x + 7.4983 R² = 0.9924	y = 55.143x + 7.0897 R² = 0.9718	y = 62.795x + 6.8098 R² = 0.9722
$V_f \cdot 10^{-7}$ /(m^3)	y = -17.116x + 0.5591 R² = 0.9816	y = -14.195x + 0.7263 R² = 0.9626	y = -19.994x + 0.8829 R² = 0.9569
$\tau \cdot 10^{-13}$ /(s)	y = 272.11x + 10.116 R² = 0.9918	y = 130.54x + 8.8252 R² = 0.9717	y = 141.8x + 7.9974 R² = 0.9729
S_n	y = -2E+09x^4 + 4E+07x^3 - 351034x^2 + 1694.3x - 0.7027 R² = 0.9614	y = -1E+10x^4 + 1E+08x^3 - 437115x^2 - 151.09x + 1.984 R² = 0.9979	y = 1E+13x^5 - 3E+11x^4 + 3E+09x^3 - 9E+06x^2 + 13958x - 5.6903 R² = 1

Table 6 — The least-square equations and regression coefficients for AS_2-13 solutions in DMF at T = (298.15, 308.15 and 318.15) K.

Parameter	Least square equations (regression coefficients, R^2)		
	T = 298.15 K	T = 308.15 K	T = 318.15 K
ρ /(kg · m^{-3})	y = 998.44x + 956.86 R² = 0.9505	y = 823.4x + 945.05 R² = 0.9606	y = 1359.7x + 930.62 R² = 0.9275
η / (mPa · s)	y = 9.1753x + 0.8445 R² = 0.9749	y = 6.6699x + 0.7574 R² = 0.9801	y = 9.4636x + 0.6299 R² = 0.9246
U / (m · s^{-1})	y = 851.1x + 1461.4 R² = 0.9827	y = 767.73x + 1422.2 R² = 0.9807	y = 879.37x + 1383.5 R² = 0.9501
$Z \cdot 10^6$ / (kg · m^{-2} · s^{-1})	y = 2.2823x + 1.3983 R² = 0.9769	y = 1.9032x + 1.344 R² = 0.9776	y = 2.7111x + 1.2875 R² = 0.9426
$\kappa_s \cdot 10^{-10}$ /(Pa^{-1})	y = -10.66x + 4.8932 R² = 0.9831	y = -10.063x + 5.2313 R² = 0.9806	y = -7.1112x + 5.5891 R² = 0.2811
$L_f \cdot 10^{-11}$ /(m)	y = -5.0639x + 4.6315 R² = 0.9831	y = -4.6312x + 4.7889 R² = 0.9809	y = -6.6984x + 4.9608 R² = 0.9457
$R_m \cdot 10^{-4}$ / (m$^{10/3}$ · s$^{-1/3}$ ·mol^{-1})	y = -6.8221x + 8.6661 R² = 0.9159	y = -5.4837x + 8.6952 R² = 0.9332	y = -10.305x + 8.7492 R² = 0.908
$b \cdot 10^{-5}$ /(m^3)	y = -7.319x + 7.5267 R² = 0.9435	y = -6.1153x + 7.6173 R² = 0.9543	y = -10.668x + 7.7318 R² = 0.9202
$\pi \cdot 10^8$ /(Pa)	y = 28.561x + 5.0647 R² = 0.9732	y = 22.732x + 4.9832 R² = 0.9796	y = 37.108x + 4.7093 R² = 0.9204
$V_f \cdot 10^{-7}$ /(m^3)	y = -21.524x + 1.6014 R² = 0.9687	y = -20.054x + 1.8122 R² = 0.9735	y = -41.696x + 2.2878 R² = 0.9019
$\tau \cdot 10^{-13}$ /(s)	y = 46.519x + 5.5121 R² = 0.9699	y = 35.425x + 5.2845 R² = 0.9672	y = 56.337x + 4.7172 R² = 0.9059
S_n	y = 3E+09x^4 - 5E+07x^3 + 313464x^2 - 316.54x + 0.2977 R² = 0.9941	y = 6E+07x^4 - 1E+07x^3 + 170862x^2 - 238.19x + 0.3697 R² = 0.9988	y = 3E+12x^5 - 7E+10x^4 + 6E+08x^3 - 2E+06x^2 + 4455.5x - 2.1395 R² = 1

Table 7 — The least-square equations and regression coefficients for AS_2-14 solutions in DMF at T = (298.15, 308.15 and 318.15) K.

Parameter	Least square equations (regression coefficients, R^2)		
	T = 298.15 K	T = 308.15 K	T = 318.15 K
ρ /(kg · m^{-3})	y = 1060.3x + 955.6 R² = 0.9685	y = 989.07x + 942.64 R² = 0.9703	y = 1730.4x + 928.44 R² = 0.9427
η / (mPa · s)	y = 7.9181x + 0.8371 R² = 0.9439	y = 7.8227x + 0.7459 R² = 0.9769	y = 10.235x + 0.617 R² = 0.9791
U / (m · s^{-1})	y = 785.23x + 1460.8 R² = 0.9792	= 672.22x + 1420.1 R² = 0.9573	y = 892.79x + 1379.5 R² = 0.97
$Z \cdot 10^6$ / (kg · m^{-2} · s^{-1})	y = 2.308x + 1.396 R² = 0.9885	y = 2.0455x + 1.3386 R² = 0.9965	y = 3.2323x + 1.2807 R² = 0.9758
$\kappa_s \cdot 10^{-10}$ /(Pa^{-1})	y = -10.55x + 4.9034 R² = 0.9919	y = -10.364x + 5.2603 R² = 0.9994	y = -17.462x + 5.6594 R² = 0.9864
$L_f \cdot 10^{-11}$ /(m)	y = -5.0143x + 4.6364 R² = 0.9921	y = -4.7471x + 4.8021 R² = 0.9993	y = -7.7477x + 4.981 R² = 0.9866
$R_m \cdot 10^{-4}$ / (m$^{10/3}$ · s$^{-1/3}$ ·mol^{-1})	y = -7.5566x + 8.6764 R² = 0.9434	y = -7.2508x + 8.7131 R² = 0.937	y = -13.745x + 8.761 R² = 0.9146
$b \cdot 10^{-5}$ /(m^3)	y = -7.8511x + 7.5366 R² = 0.964	y = -7.505x + 7.6366 R² = 0.9658	y = -13.743x + 7.7496 R² = 0.938
$\pi \cdot 10^8$ /(Pa)	y = 25.428x + 5.0386 R² = 0.9463	y = 27.329x + 4.9407 R² = 0.971	y = 41.387x + 4.6609 R² = 0.9719
$V_f \cdot 10^{-7}$ /(m^3)	y = -19.282x + 1.6233 R² = 0.9325	y = -24.457x + 1.8492 R² = 0.9617	y = -46.154x + 2.3444 R² = 0.9627
$\tau \cdot 10^{-13}$ /(s)	y = 38.838x + 5.4748 R² = 0.916	y = 43.447x + 5.2334 R² = 0.9608	y = 60.389x + 4.6596 R² = 0.9672
S_n	y = 3E+09x^4 - 5E+07x^3 + 288921x^2 - 285.29x + 0.311 R² = 0.9949	y = 4E+08x^4 - 7E+06x^3 + 37143x^2 + 330.5x + 0.0534 R² = 0.9883	y = -5E+12x^5 + 1E+11x^4 - 9E+08x^3 + 3E+06x^2 - 4029.9x + 2.7071 R² = 1

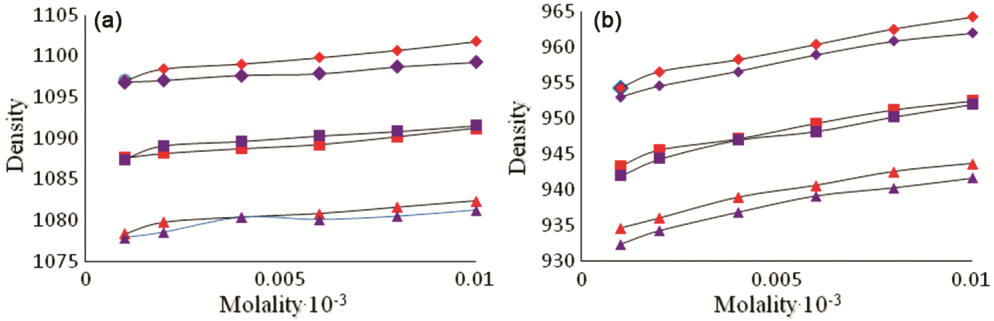

Fig. 2 — The plots of Density (ρ) against molality (m) for AS_2-13 and AS_2-14 in (a) DMSO and (b) DMF at 298.15K [AS_2-13-(♦), AS_2-14-(♦)], 308.15K [AS_2-13-(■), AS_2-14-(■)] and 318.15K [AS_2-13-(▲), AS_2-14-(▲)].

Ultrasonic sound velocity (U) is inversely proportional to intermolecular free path length (L_f). Table 4, Table 5, Table 6 and Table 7 demonstrate that in the DMSO and DMF systems, the ultrasonic sound velocity (U) and acoustical impendence (Z) of the solutes both increased with C and decreased with T. The structural configuration of both derivatives was significantly changed as result of solvent-solute interactions. As shown in Table 4, Table 5, Table 6 and Table 7, the intermolecular free path length (L_f) was observed to increase with T and decrease with C for both derivatives, indicating the possibility of solvent-solute interactions. The system's distribution of U provides information about the typical duration of the relaxation process that results in the distribution. Procedures for structural relaxation were the cause of the detected viscous relaxation time (τ).The viscous relaxation time (τ) of the mixture decreased with T and increased with C in both binary systems.

The encircling of solute molecules with solvent molecules, supporting strong solvent-solute interactions in both binary mixtures may be the cause of the isentropic compressibility (K_S) increasing with

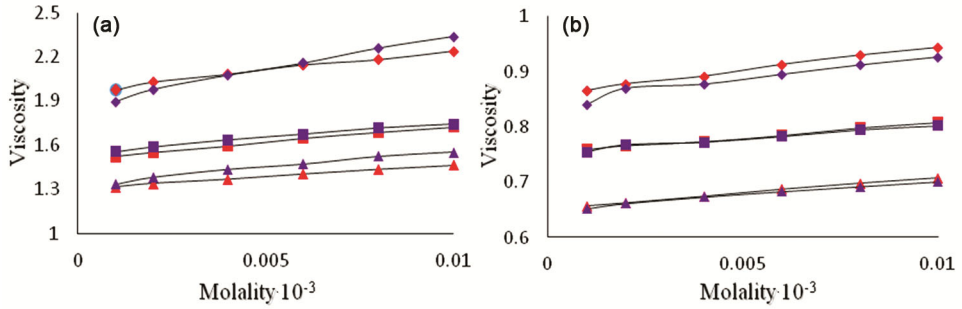

Fig. 3 — The plots of Viscosity (η) against molality (m) for AS_2-13 and AS_2-14 in (a) DMSO and (b) DMF at 298.15K [AS_2-13-(♦), AS_2-14-(♦)], 308.15K [AS_2-13-(■), AS_2-14-(■)] and 318.15K [AS_2-13-(▲), AS_2-14-(▲)].

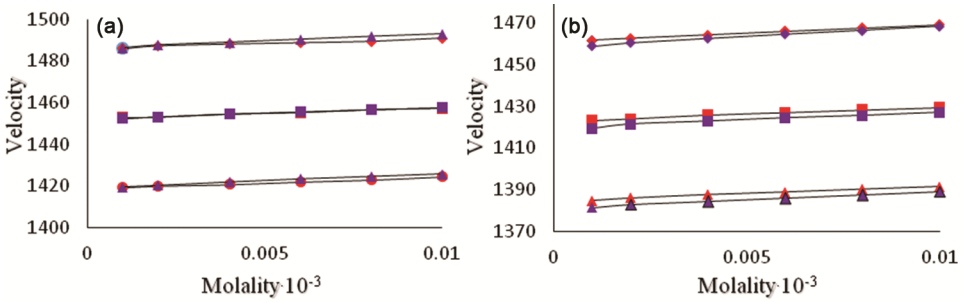

Fig. 4 — The plots of Velocity (U) against molality (m) for AS_2-13 and AS_2-14 in (a) DMSO and (b) DMF at 298.15K [AS_2-13-(♦), AS_2-14-(♦)], 308.15K [AS_2-13-(■), AS_2-14-(■)] and 318.15K [AS_2-13-(▲), AS_2-14-(▲)].

T and decreasing with *C*. The solvated molecules that were completely compressed by the electrical forces are to blame for this phenomenon.

The linear fluctuations in Rao's molar sound function (R_m) and Van der Waals constant (b) shown in Table 4, Table 5, Table 6 and Table 7, (correlation coefficient R^2 = 0.831-0.999) propose that complex or aggregate formation taken place for AS_2-13 and AS_2-14 in DMSO and DMF systems. The forces of attraction and repulsion that develop between the entities in the solution are what lead to internal pressure (π). For compounds AS_2-13 and AS_2-14, The intermolecular free path length and isentropic compressibility results demonstrated a decrease with C and an increase with *T*. This was established from the results of internal pressure (π), which was found enlarged. A solute molecule's free volume (Vf) at a given temperature and pressure is determined by the internal pressure of the liquid in which it is dissolved. In both the binary systems, an increase in internal pressure (π) and a decrease in free volume (V_f) indicates an increase in cohesive forces *vice versa*.

Relationships of solvation number were another way to quantify the degree of interaction (S_n). The significance of the Sn is determined by solvent-solute and solute-solute interactions *Sn*. The results show that Sn values increased nonlinearly with C and decreased with T. Positive *Sn* values indicate a structure-forming tendency of AS_2-13 and AS_2-14 in both binary systems. Strong dipole-dipole interactions were also suggested by the difference in *Sn* with *C* and *T* values.

Conclusions

The purpose of the current analysis was to assess the importance of the solution study. At three different temperatures 298.15, 308.15 and 318.15 K, these variables were used to calculate the solute-solvent and solute-solute interaction and at atmospheric pressure. The behavior of compounds AS_2-13 and AS_2-14 in DMSO and DMF was associated on the basis of their structures. AS_2-13 possesses -NO_2 group, which is an electron-withdrawing group in nature and AS_2-14 possesses -NH_2 group, which is electron-donating group in nature and –NO_2 group is highly electronegative compared to -NH_2 group, Because of this, it was sometimes discovered that the behaviour of both the derivatives in DMSO and DMF was different. This resulted from the fact that both groups were crucial in molecular interactions. On the basis of positive values for the solvation number, the structure formed as a result of significant molecular interactions. The conclusion drawn from the experimental data is that ρ,

η and U increased with concentration and decreased with temperature. The various thermo-acoustical factors determined in this work support the existence of weak and strong dispersive powers in binary mixtures. This study also reveals that 1*H*-benzo[*d*]-imidazol substituted 1,3,4-oxadiazole derivatives acts as a structure former in the binary systems considered.

Acknowledgement

The authors thank the Department of Chemistry and M. K. Bhavnagar University for providing facilities. Authors are also thankful to CSIR-CSMCRI Bhavnagar for providing instrumental facilities and Anwar H. Saiyad is thankful to the University Grants Commission, New Delhi for providing a JRF fellowship [No. JUNE18-103309].

Disclosure statement

No potential conflict of interest was reported by the authors.

Funding

This research did not receive any specific grant from funding agencies in the public, commercial, or not-for-profit sectors.

References

1 Naik R R & Bawankar S V, *Russ J Phys Chem A*, 89 (2015) 2388.
2 Kumar R, Swarnalatha N, Mahesh R, Shanmugapriyan B & Kannappan V, *J Mol Liq*, 163 (2011) 57.
3 Schneider J, Kienzler A, Deuchert M, Schulze V, Kotschenreuther J, Zum Gahr K H, Löhe D & Fleischer J, *Microsyst*, 14 (2008) 1797.
4 Gogate P R, *Curr Opin Chem Eng,* 17 (2017) 9https://doi.org/10.1016/j.coche.2017.05.003.
5 Hoffmann M R, Hua I & Höchemer R, *Ultrason Sonochem*, 3 (1996) S163.
6 Gupta S, Dandia A, Singh P & Qureishi M, *J Mater Einviron Sci*, 6 (2015)168.
7 Nozdrev V F, Application of ultrasonics in molecular physics. Gordon and Breach, (1963).
8 Pierce A D, *Acoustics*, (McGraw-Hill. New York) 1981, p. 481.
9 Koh L L, Nguyen H T, Chandrapala J, Zisu B, Ashokkumar M & Kentish S E, *J Memb Sci*, 453 (2014) 230.
10 Rathnam M V, Sayed R T, Bhanushali K R & Kumar M S*, J Mol Liq*, 166 (2012) 9.
11 Godhani D R, Jogel A A, Mulani V B, Sanghani A M, Kukadiya N B & Mehta J P, *AJRC*, 11(2018) 32.
12 Godhani D R, Dobariya P B, Sanghani A M, Jogel A A & Mehta J P, *J Mol Liq*, 180 (2013) 179.
13 Mehta J P, Pandya K I & Godhani D R, *J Chem Thermodyn*, 70 (2014) 33.
14 Roy M N, Dakua V K & Sinha B, *Int J Thermophys*, 28 (2007) 1275. https://doi.org/10.1007/s10765-007-0220-0
15 Kanhekar S R & Bichile G K, *J Chem Pharm Res*, 4 (2012) 78.
16 Pandiyan V, Vasantharani P, Oswal S L, Malek N I & Vasantharani P, *J Chem Eng Data*, 56 (2011) 269.
17 Mastrobattista E, Koning G A & Storm G, *Adv Drug Deliv Rev*, 40 (1999) 103.
18 Vane J R & Botting R M, *J Inflamm Res*, 47 (1998) 78.
19 Schechter L E, Ring R H, Beyer C E, Hughes Z A, Khawaja X, Malberg J E, & Rosenzweig-Lipson S, *NeuroRx*, 2 (2005) 590.
20 Biot C, Glorian G, Maciejewski L A Brocard J S, Domarle O, Blampain G, Millet P, Georges A J, Abessolo H, Dive D & Lebibi J, *J Med Chem*, 40 (1997) 3715.
21 Pandeya S, Sriram D, Nath G & DeClercq E, *Eur J Pharm Sci*, 9 (1999) 25.
22 Padmavathi V, Thriveni P, Reddy G S & Deepti D, *Eur J Med Chem*, 43 (2008) 917
23 Tanitame A, Oyamada Y, Ofuji K Fujimoto M, Iwai N, Hiyama Y, Suzuki K, Ito H, Terauchi H, Kawasaki M & Nagai K, *J Med Chem,* 47 (2004) 3693.
24 Park K D, Cho S J, Moon J S & Kim S U, *Bioorg Med Chem Lett*, 20 (2010) 6551.
25 Meade E A, Wotring L L, Drach J C& Townsend L B, *J Med Chem*, 35 (1992) 526.
26 Manickam M, Ramanathan M, Farboodniay Jahromi M A, Chansouria J P & Ray A B, *J Nat Prod*, 60 (1997) 609.
27 Tanaka H, Takashima H, Ubasawa M, Sekiya K, Inouye N, Baba M, Shigeta S, Walker R T, De Clercq E & Miyasaka T, *J Med Chem*, 38 (1995) 2860.
28 Bonsignore L, Loy G, Secci D & Calignano A, *Eur J Med Chem,* 28(1993) 517.
29 Bagchi S, Nema S K & Singh R P, *Eur Poly J*, 22 (1986) 851.
30 Vigoureux P, *Ultrasonic*, (*Chapmann and Hall* London), 1952).
31 Suryanarayana C V, *J Acoust Soc Ind*, 131 (1979).
32 Surayanarayana C V & Kuppusami J, *J Acoust Soc India*, 4 (1976) 75.
33 Jacobson B, Anderson W A & Arnold J T, *Nature*, 173 (1954) 772.
34 Shekaari H, Bezaatpour A & Soltanpour A, *J Chem Eng Data*, 55 (2010) 5927.
35 Gokavi G S, Raju J R, Aminabhavi T M, Balundgi R H & Muddapur M V, *J Chem Eng Data*, (1986) 8.
36 Keshapolla D & Gardas R L, *Fluid Ph Equilibri*a, 383 (2014) 32.
37 Papamatthaiakis D, Aroni F & Havredaki V, *J Chem Thermodyn*, 40 (2008) 107.
38 Syal V K, Patial B S & Chauhan S, *Ind J Pure Appl Phys,* 37 (1999) 366.
39 Pal A & Kumar A, *J Chem Eng Data*, 50 (2005) 856.
40 Baluja S & Shah A, *Fluid Ph Equilibria,* 215 (2004) 55.